DESIGN OF ELECTROMAGNETIC BEARING FOR VIBRATION

CONTROL OF FLEXIBLE TRANSMISSION SHAFT*

V. Gondhalekar
E.T.H. Zürich, Switzerland

R. Holmes
Department of Mechanical Engineering
University of Southampton, U.K.

Recently magnetic bearings have been proposed by several researchers and shown to be viable on a variety of rotor assemblies. This paper is concerned with the design and construction of such a bearing, which employs features hitherto not used by other workers. These include an original approach to the design of the electromagnets and their amplifiers, and to software in a digital control system, to condition the control signals so as to make the magnets appear to be linear and uncoupled. The resulting system is used to control a rotor-bearing assembly, whose speed range covers two flexural-critical speeds.

INTRODUCTION

The feasibility of using magnet forces to control shaft vibrations has recently been a subject of attention from a number of researchers and successful application of bearings and dampers in rotating assemblies has been reported [1,2,3]. A flexible transmission shaft is a special case of a rotating assembly which needs some form of control to maintain its vibration amplitudes within reasonable limits when passing through its critical speeds. Squeeze-film bearings have been shown to be capable of reducing vibration amplitudes but these can normally only react to the rotor displacement at the bearing locations. A controlled electromagnet (CEM) located at a point along the length of a transmission shaft has also been shown to be effective in reducing vibration amplitudes [2]. The CEM offers the possibility of applying a force which is a function of displacement and/or velocity at the CEM location or at a location remote from it. This offers the possibility of implementing a control strategy which responds to one signal or to the weighted average of more than one signal measurement remote from the CEM location.

Some magnetic bearing configurations proposed by past workers are shown in Fig.1. The static member of that shown in Fig.1a is the simplest to construct but in an attempt to combat eddy current effects the rotating sleeve must be made from

rectangular laminations. Any lamination completing the flux path only does so for a short time increment and other laminations sequentially perform this function as the shaft rotates. A relatively long axial length is needed to provide a given magnetic force. The radial flux configuration of Fig.1b makes lamination of both the static and rotating members easy, the latter now being constructed from flat discs. A disadvantage, however, is inefficient radial space utilization. Also the long narrow limbs lead to high magnetic saturation, that is high flux concentration at the magnet bases.

Magnetic bearings are best designed to operate in an attraction rather than a repulsion mode, but in either case the basic inverse square-law relationship between magnetic force and gap has to be overcome since this can lead to instability. Schweitzer [1] describes a design similar to that of Fig. 1b in which stability is achieved, together with the linearity of the force-current characteristic by a differential circuit, in addition to a circuit ensuring premagnetisation with a constant current. Thus operation takes place about a non-zero steady-state condition. Easier analysis and controller design are assured by the improvement in linearity but bulky magnets are necessary to dissipate the consequent heat produced by the premagnetisation current.

A logical next step is to integrate all four magnets into a single structure as shown in Fig. 1c. However, there is here a high degree of interaction between the four poles, and consequently the magnet performance has to be improved by special techniques requiring bidirectional drive amplifiers to alter the direction of the flux as required [2]. This disadvantage can be overcome by using the four active/four passive pole configuration of Fig. 1d [3], in which four unidirectional amplifiers can be used.

Fig. 1e shows a 3 pole active/3 pole passive configuration as used in the present work, as it gives a better space utilization than does that of Fig. 1d, as well as reducing magnet interaction. However, since the magnets do not lie on mutually perpendicular axes, xy, cross-coupling is introduced between these axes. This is counteracted by suitable software using a microprocessor interface which in any case is essential for adaptive control purposes. Also it was decided to design for operation about a point of zero magnet excitation as this obviates the need for an extra coil to supply a constant magnetising current. Thus resistive heating of the magnet coils is reduced and consequently their weight and size. The whole device is required to exert dynamic rather than static force components and hence there is no need from that point of view for a non-zero quiescent operating point. One of the main objectives of the present work is to design software to condition the control signals so as to make the magnets appear linear (and uncoupled) in spite of using this zero-excitation

operating point.

The rotor system controlled by the electromagnets is shown in Fig.2, and the final electromagnet configuration in Fig.3. The overall system including the microprocessor and associated peripherals is shown in Fig.4. The electromagnets, their drive electronics and the computer system are described in some detail and some results obtained from the rig to date are presented.

THE ELECTROMAGNETS AND THEIR DRIVE ELECTRONICS

A block diagram of the electromagnet system designed for the present work is shown in Fig.5. Each power amplifier, A, which drives a magnet coil, C, is of the switching type, employing pulse-width modulation to reduce power losses. It is designed to operate at a maximum A.C. input of 220 v rms and as a result approximately 300 v D.C. is available to drive each coil, with a current limit of 10 amp, but with available capacity up to 15 amp.

The electromagnet configuration of Fig.3 consists of six radial poles - 3 active and 3 passive - the latter acting as return flux paths. The electromagnets and the rotor sleeve are constructed from 0.1 mm disc laminations to eliminate eddy currents up to approximately 300 Hz and the 3 active poles were suitably energised to generate forces along the x and y axes. This particular configuration was chosen because it utilizes the available radial space more efficiently in terms of force than a similar structure consisting of four active poles, and the number of drive amplifiers is reduced from 4 to 3. One disadvantage is the force interaction introduced between the orthogonal axes, but as mentioned above, software is employed to overcome this problem.

An electromagnet exerts a force approximately proportional to the square of the magnet flux present at the pole face. It is also unstable in an open loop mode since, as the deflection increases towards a magnet, so does the attractive force from that magnet. The system can, however, be made stable by feeding back a signal v_H produced by a Hall probe, which is proportional to the flux at the pole face (Fig.5).

Since the electromagnets can only operate effectively in an attraction mode, with no repulsion, then in order to overcome this unidirectional forcing feature in creating restoring forces to counteract displacements, X and Y, the excitation signals, S_1, S_2, S_3, to the three drive amplifiers A (Fig.5) would be constituted as follows:

$$S_1 = [Y]_{T/2}^T - 0.5[X]_0^{T/4} + 0.5[X]_{T/4}^{3T/4} - 0.5[X]_{3T/4}^T$$

$$S_2 = -[Y]_0^{T/2} - [X]_0^{T/4} - [X]_{3T/4}^T \qquad (1)$$

$$S_3 = - [Y]_0^{T/2} + [X]_{T/4}^{3T/4}$$

where T is the periodic time. For displacements X and Y as shown in Fig. 6a, the signals S thus appear as shown in that figure.

It will be noted that all three signals contain both X and Y components. This is because magnets 2 and 3 have to exert forces to counter X and Y displacements, but in the process introduce unwanted X-dependent forces in the Y direction. These are neutralised by additional X-component forces generated in magnet 1 by signal S_1. Assuming that a linear relationship exists between the signals and the attraction forces produced by the magnets, then, for some amplifier gain, C,

$$F_y = C[-S_1 + (S_2 + S_3)\cos 60°]$$

$$F_x = (2C/\sqrt{3})[(S_2 - S_3) \cos 30°].$$

In fact, the force produced at each pole face is proportional to the square of the flux at that face and hence to the square of the current supplied to each magnet coil. Thus, if there is a linear relation between any signal S and its coil current then each magnet force will be proportional to S^2 and not to S as assumed above. However, this can be partially accommodated by replacing the multiplier 0.5 in the first of equations (1) by 0.5, the other two equations remaining unaltered. This is followed by writing F_y and F_x as

$$F_y = [-(S_1)^2 + [(S_2)^2 + (S_3)^2] \cos 60°]C$$

$$F_x = \{[(S_2)^2 - (S_3)^2] \cos 30°\}(2C/\sqrt{3})$$

As a result, the forms of the forces produced in the x,y directions are shown in Fig. 6b. When combined to produce a

polar force diagram a signficant 3rd Harmonic is revealed (Fig.6c).

Linearisation of each magnet device can, however, be achieved by using the square root of the control signal input, S, to each magnet amplifier. This input signal then produces a proportional flux, the approximate square of which is proportional to the force exerted on the rotor. The control signal S, vs force output thus follows an approximately linear relationship and allows the signal and hence force contributions of the three magnets to be added linearly.

The square root of a number can be found using software by computing a finite number of terms of a series expansion, but this can be time-consuming in a real-time application. A piece-wise linear approximation to the function $y = K\sqrt{S}$ was therefore used, where S is the control signal, and K is a constant. The above function is divided into 32 segments of progressively greater length, since a square root function varies rapidly around zero, and the software computes the square root in 96 μsec on a Z8002 cpu. The square-rooting procedure, when applied to the control signals of all 3 magnets results in the polar force diagram shown in Fig. 6d, indicating considerable improvement over that shown in Fig. 6c. The software can be adapted, if required,to compensate for the saturation of the magnet core material also.

As well as being influenced by the square-law non-linearity, the magnet forces are also subject to current-rate saturation in the drive amplifiers. This occurs if more than the maximum drive voltage of the amplifier is demanded. Fortunately, in practice, the current rates demanded are low enough to be unaffected by any limitations in V, particularly when the restoring forces provided by the magnets are kept within reasonable limits.

CONTROL STRATEGY

Assuming negligible internal damping, the rotor vibration can be represented by the following set of equations:

$$y_i = \sum_{j=1}^{j=3} \alpha_{ij}(P_j + m_j\omega^2 y_j) - \alpha_{i4}K_d y_4, \quad i = 1 \text{ to } 4$$

where α_{ij} are the influence coefficients (m/N) relating to the mass stations 1, 2 and 3, ω is the rotor speed in rad/s, P_j are the forces due to mass unbalance, y_j are displacement amplitudes at the mass stations and K_d is the stiffness introduced by the CEM at station 4. The negative dynamic stiffness curve at station 4 for this rotor is shown in Fig.7. Dynamic stiffness is the rotor dynamic force at station 4

355

divided by dynamic displacement, and the frequencies at which the negative stiffness equals the dynamic stiffness of the support at station 4 are the natural frequencies of the complete system. Thus the intersections with a horizontal line K_d parallel to the ω-axis give the natural frequencies ω_n (that is critical speeds) of the rotor system. A speed-dependent controller can ensure that the natural frequencies of the rotor system are sufficiently removed from the mass-unbalance disturbance frequency (that is the rotational speed) by automatically adjusting the stiffness K_d.

It is also possible to introduce both stiffness and damping at station 4. Fig. 8 shows some typical response curves taken from the rotating assembly of Fig.2, sample values of stiffness and damping provided by the controlled electromagnets being indicated. These serve to indicate how the critical speeds can be altered and the peak responses brought down to acceptable levels.

CONCLUSIONS

The results of this research indicate that efficient and compact electromagnets have been designed to effectively control the vibrations of a supercritical rotating assembly. By the use of a microprocessor, software has been designed to overcome any problems of cross-coupling between orthogonal axes and of inherent non-linear force-deflection characteristics in the magnets. By the same microprocessor a considerable degree of control can also be achieved, as indicated in Fig. 8.

REFERENCES

1. Schweitzer, G. and Ulbrich, H. 'Magnetic Bearings - a novel type of suspension'. I.Mech.E. Conference on Vibrations in Rotating Machinery, Cambridge, Sept. 1980.

2. Nikolajsen, J.N., Holmes, R. and Gondhalekar, V. 'Investigation of an electromagnetic damper for vibration control of a transmission shaft'. Proc. I.Mech.E. Vol. 193, No.31, 1979.

3. Habermann, H. 'Le Palier magnetique actif "ACTIDYNE"'. AGARD Conference Proceedings, No. 323, 'Problems in Bearings and Lubrication', Ottawa, Canada, May 1982.
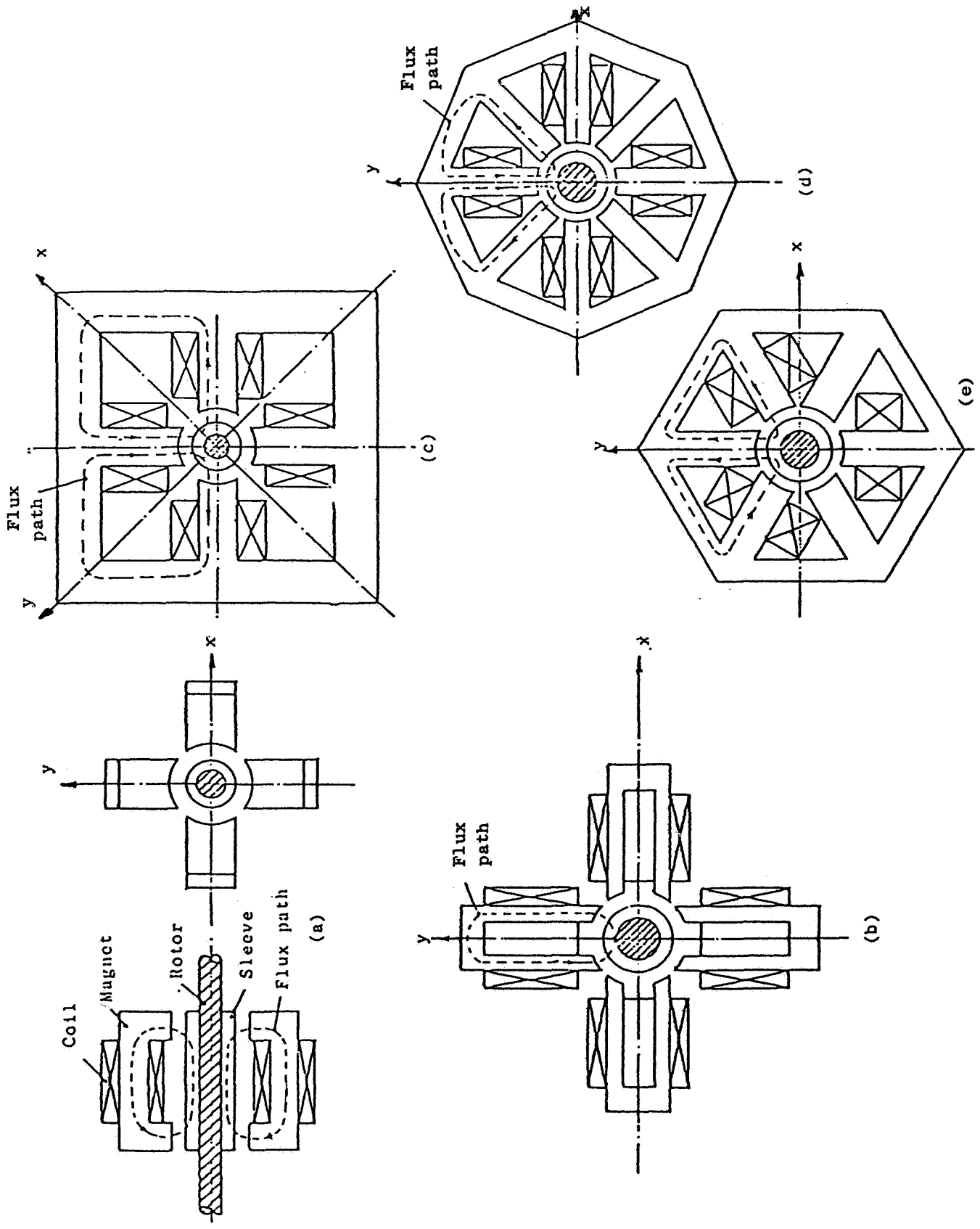
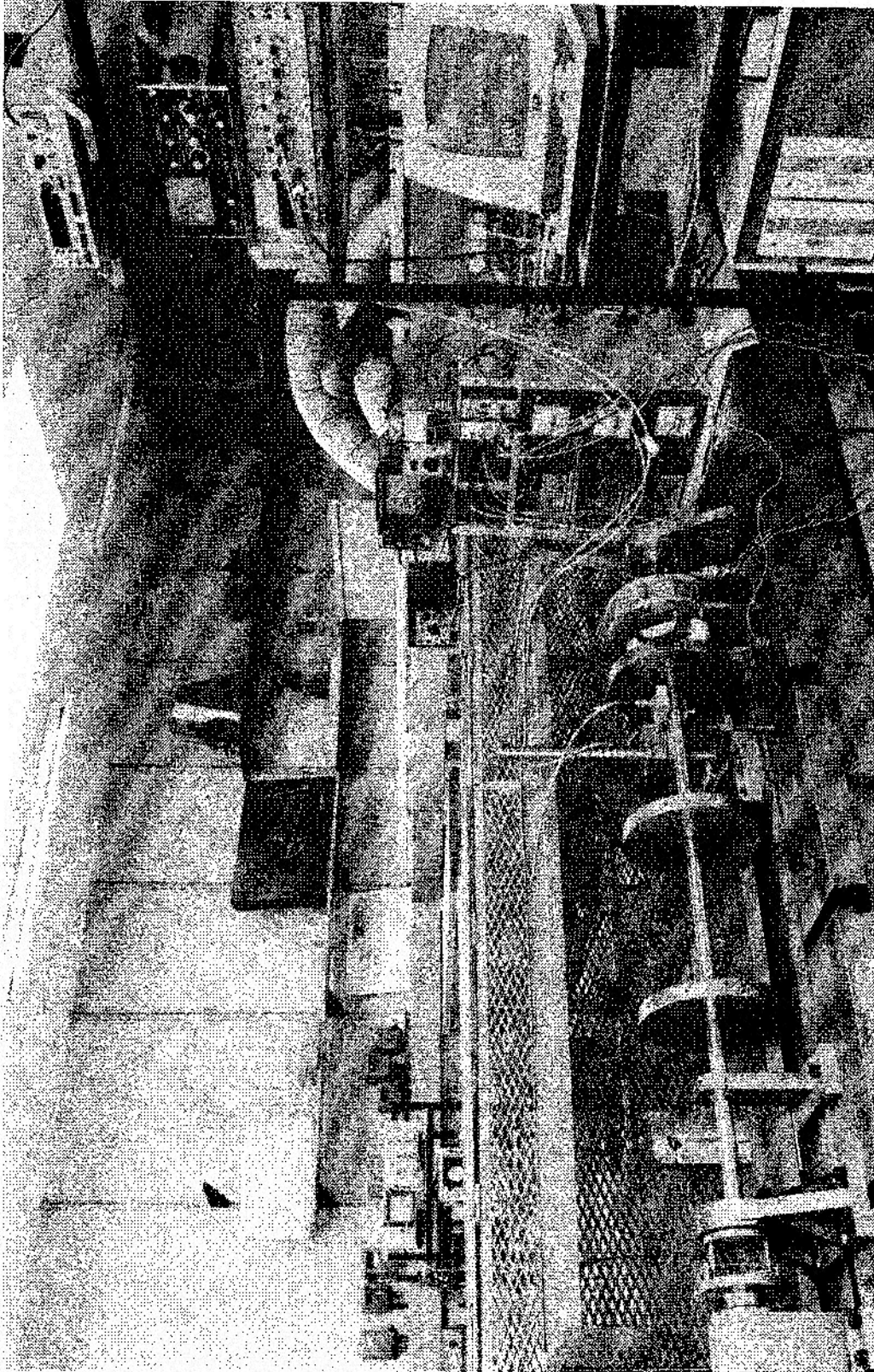Figure 1. – Viable magnetic bearing configurations.

357

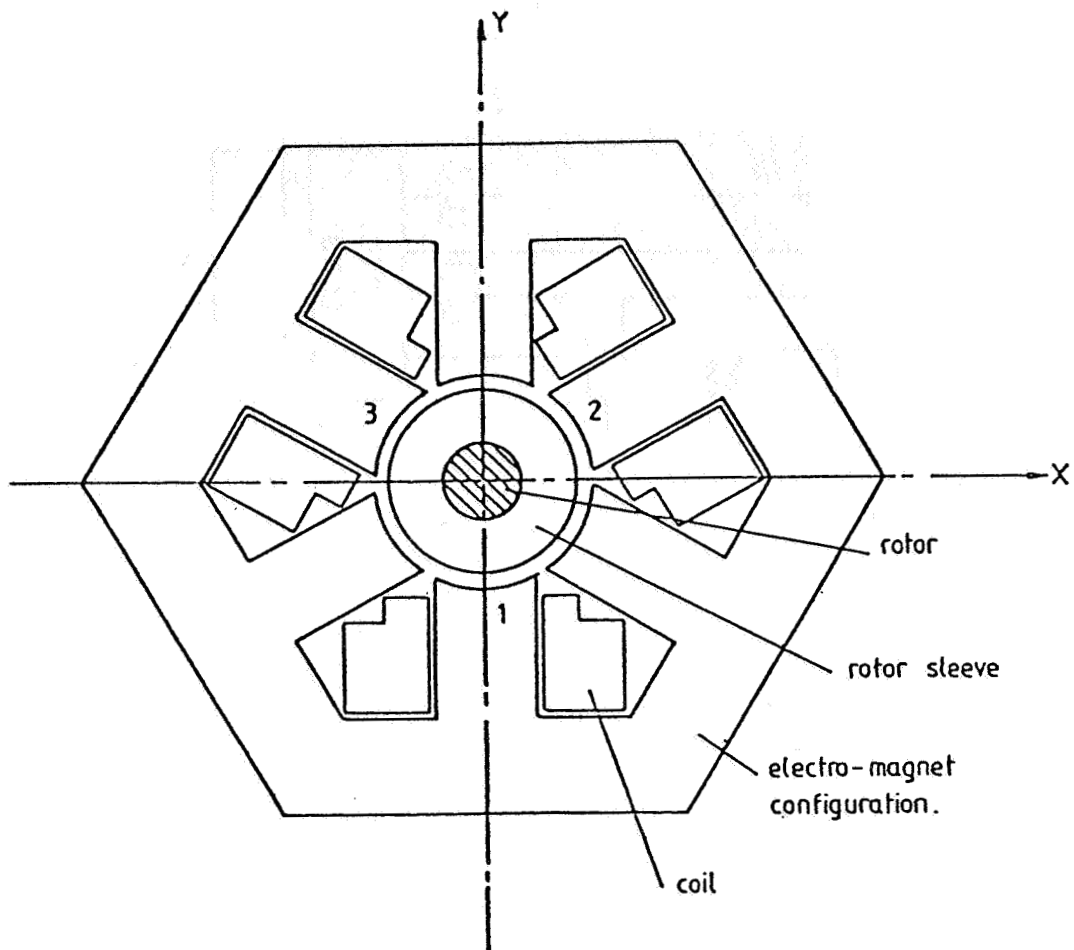Figure 2. - Rotor and electromagnetic device. Span, 1.265 m; total mass, 30 kg.

Figure 3. - Active-pole electromagnet configuration. Radial air gap, 2 mm; radial stiffness, 1×10^5 to 10×10^5 N/m; peak power requirement, 200 W.
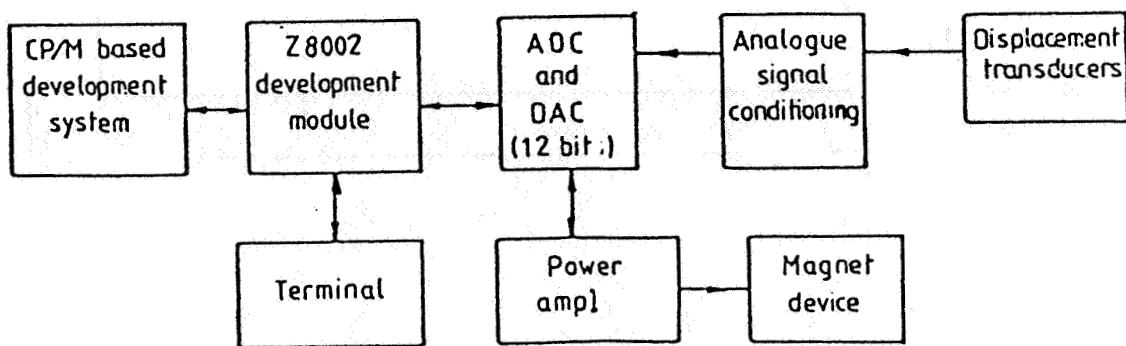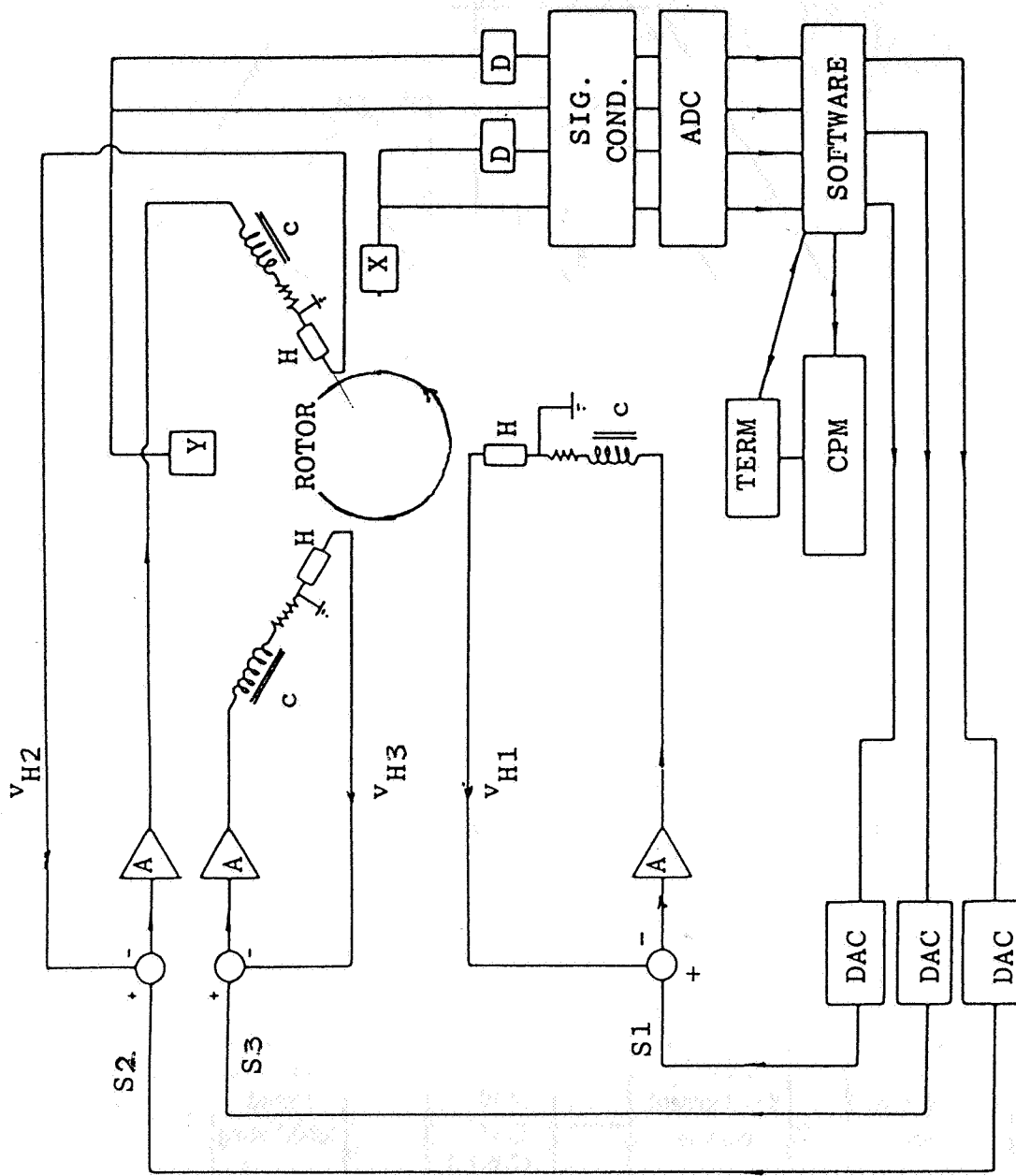
Figure 4. - Computer and electromagnet system.
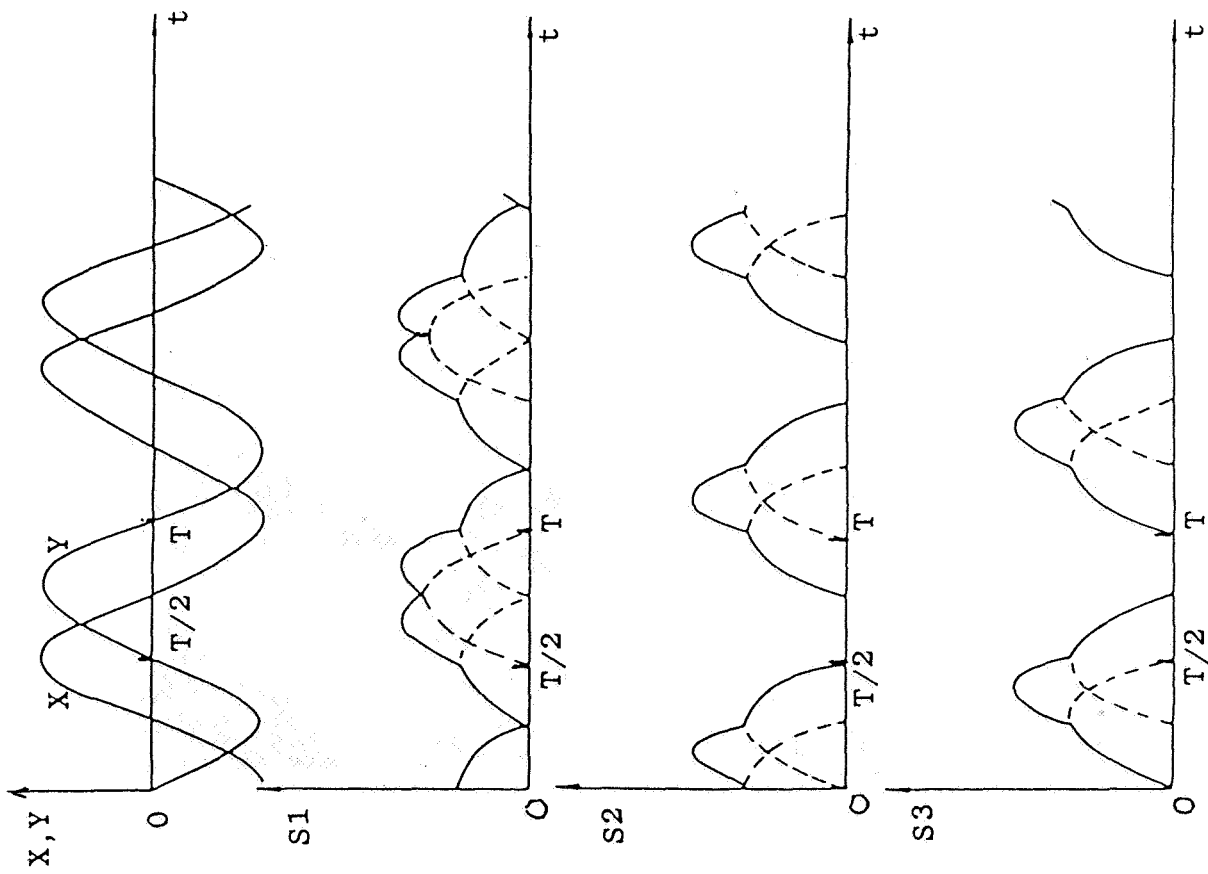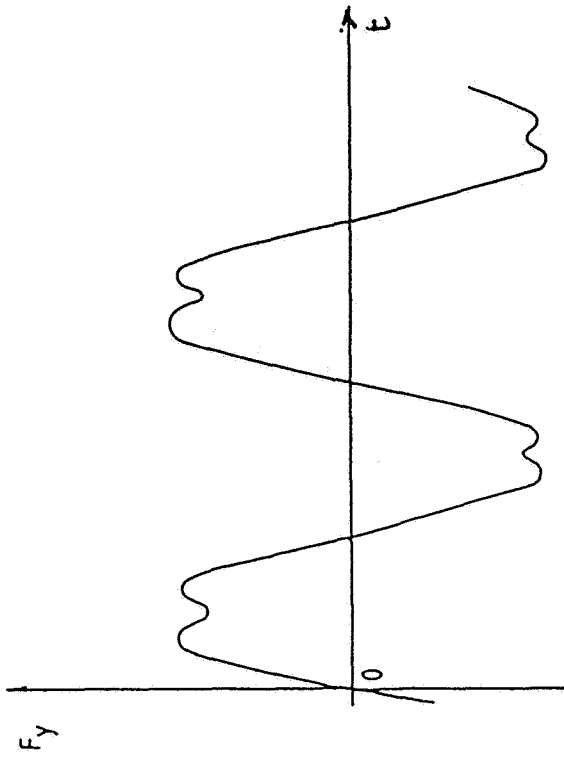
Figure 5. – Electromagnet system.

Figure 6b. - Forces in orthogonal directions.

Figure 6a. - Excitation signals.
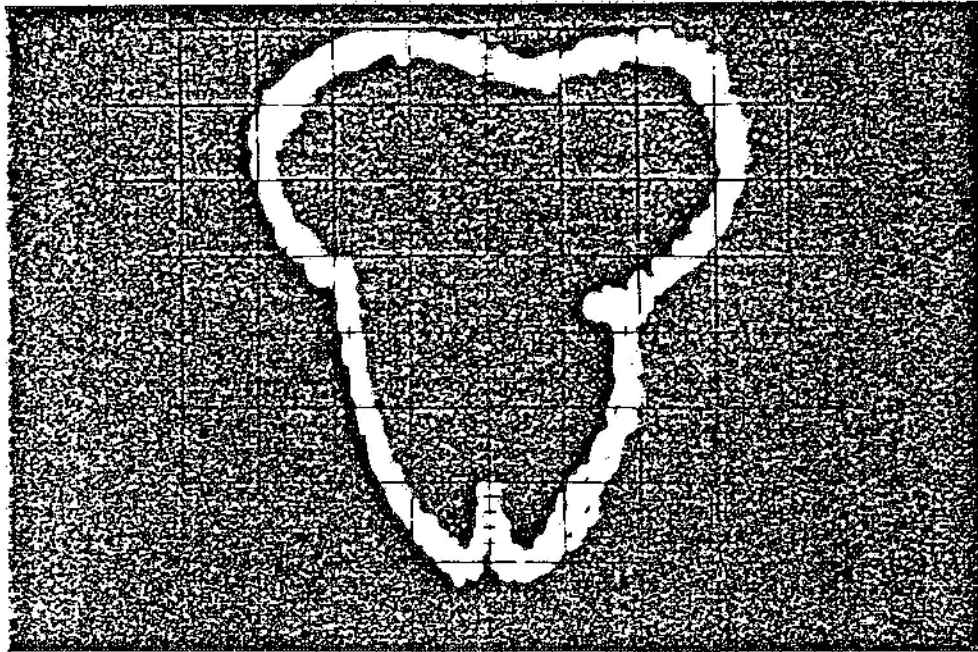
Figure 6c. - Polar force diagram.
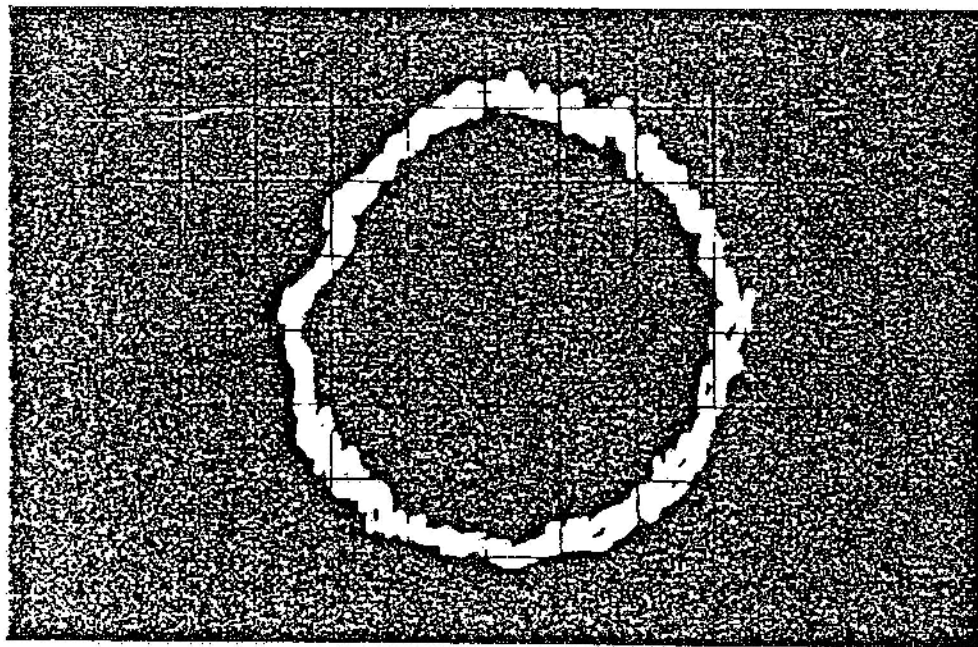
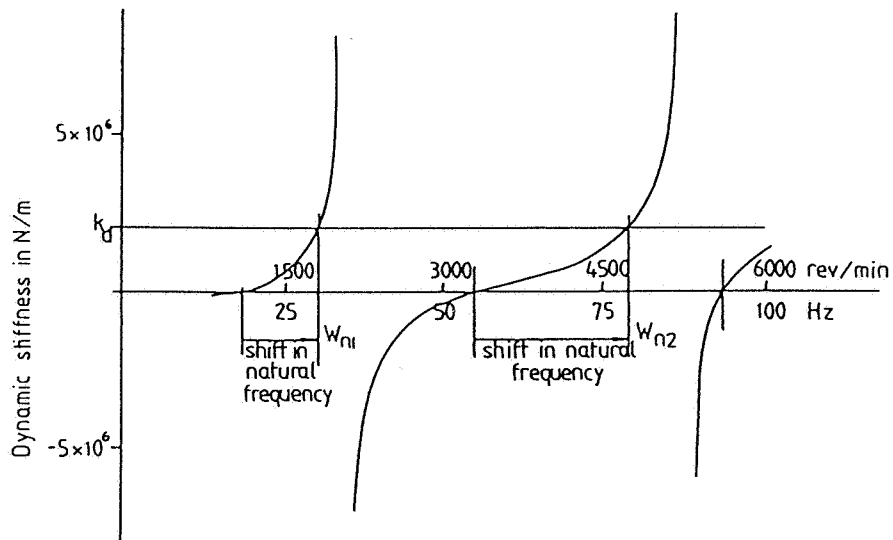Figure 6d. - Improved polar force diagram.

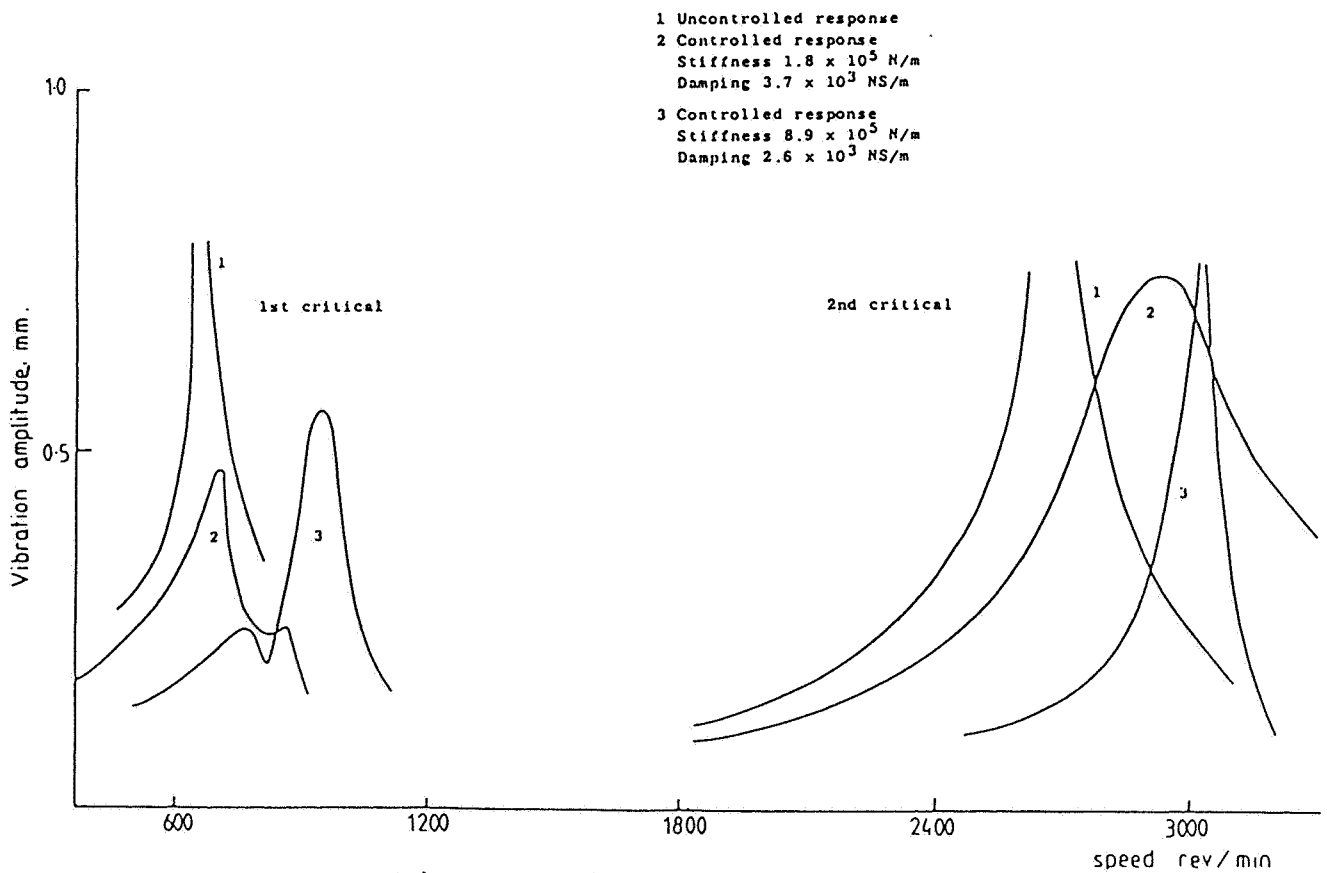Figure 7. - Negative dynamic stiffness curve and shifts in natural frequency due to k_d.

Figure 8. - Typical response curves.